JOURNAL OF APPLIED ELECTROCHEMISTRY 2 (1972) 113–122

Electrochemical removal of copper ions from very dilute solutions

DOUGLAS N. BENNION

Department of Energy and Kinetics, School of Engineering and Applied Science, University of California, Los Angeles, U.S.A.

and

JOHN NEWMAN

Inorganic Materials Research Division, Lawrence Berkeley Laboratory, and Department of Chemical Engineering, University of California, Berkeley, U.S.A.

Received 23 September 1971

A device for concentrating electropositive cations using porous, fixed, flow-through, carbon electrodes is described. A feed of 667 μg of copper per ml of solution was reduced to less than 1 μg of copper per ml of solution. The flow rate was 0·20 $cm^3/cm^2/min$ through a bed 6 cm thick. Capital cost for the cell is the controlling factor. A preliminary economic analysis indicates that the value of copper recovered will more than pay for the installation and operation of the cell, even for fairly small units.

Introduction

In many industrial waste streams there are metal ions which can be toxic to plant and animal life even at concentrations in the order of 1 μg/ml. Some examples are copper, mercury, lead, arsenic, and cadmium. Copper is toxic to trout at the 0·14 μg/ml level [1].

There are at least four methods in use or being tested for removing copper ions. The copper can be exchanged for iron by running the waste stream through a packed bed of iron. In this method, the effluent will be enriched with iron, the mass transfer of copper ions to the iron surface and transfer of iron ions from the surface will be impeded as a layer of copper forms on the iron, and the spent bed (mixed copper and iron) must be mechanically removed and new iron put in periodically. A second method is to increase the pH of the waste stream above 7 by adding calcium oxide or other base and precipitating hydrated copper oxide. The floc must then be settled, concentrated, and the copper recovered using standard sludge handling procedures. A third technique is to run the waste stream through a fixed bed of ion exchange resin [2]. This method has been used successfully to recover uranium, gold, platinum, mercury, and chromates. Resins are now becoming available for removing copper. The resins constitute a major contribution to the capital cost, and in some cases the spent resin cannot be regenerated. A fourth technique is to plate copper electrochemically onto particles in a fluidized bed as described by Fleischmann *et al.* [3].

The use of porous, fixed, flow-through electrodes as a means of removing metal ions is reported on here. This porous-electrode technique bears some resemblance to the ion-exchange method and the fluidized-bed method. However, inexpensive flakes and chips of carbon and graphite can be used as the porous electrodes, i.e., both anode and cathode, and the electrodes can be regenerated in place. The porous electrodes are arranged with the cathode over the anode (see Fig. 1). The feed enters the region

C

between the electrodes. About 99% of the flow passes up through the cathode. Copper is plated out on the surface of the carbon bed, and purified effluent goes out the top. When the cathode is filled to capacity with copper, the electrodes are inverted, i.e., the cell is turned upside down, and the copper-filled electrode becomes the anode. About 1% of the inlet flow

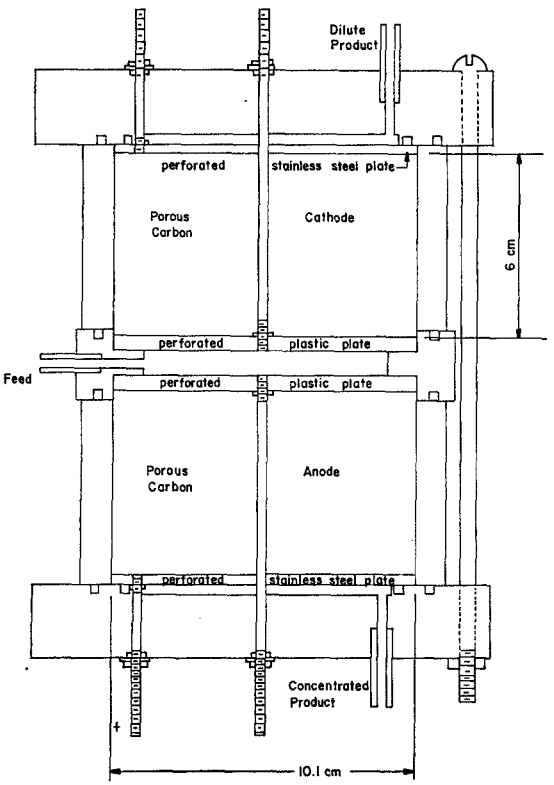

Fig. 1. Copper ion removal and concentrating cell.

goes through the anode. Copper ions are electrochemically added to the anolyte. Thus, the bottom effluent is highly enriched in copper ions. The copper can then be recovered in an electrowinning cell or other copper reduction process.

Design Principles

The principal cell design objective is the reduction of the copper ion concentration from about 600 μg/ml in the feed to 1 μg/ml or below in the catholyte effluent. The ion removal takes place in the porous cathode. Thus, the size and cost of the complete cell is controlled by the size of the porous cathode. In order to remove the maximum amount of copper in a minimum volume, a high surface area bed with a maximum mass-transfer driving force for the copper ions is needed. The high surface area is realized by using finely divided graphite chips or flakes. The maximum driving force is achieved by operating so that the copper concentration at the surface of the graphite is close to zero, i.e., limiting current.

The longer the effective contact time, the greater will be the separation factor, i.e., the copper concentration of the feed divided by the catholyte effluent concentration, c_0/c_b^L. The contact time is inversely proportional to the catholyte flow rate and proportional to the cathode thickness. Higher flow rates can be used for a thicker cathode.

Another design criterion is that hydrogen evolution not occur within the cathode. The potential in the solution at the exit to the cathode, Φ_2^L, must be sufficiently positive to insure limiting current for the copper ions there. The copper deposition throughout the porous cathode implies an electric current and therefore a potential drop in the catholyte, $\Delta\Phi_2 = \Phi_2^L - \Phi_2^0$. When the potential in the front of the electrode, Φ_2^0, becomes sufficiently positive, hydrogen evolution will occur. Higher flow rates imply larger electric currents and a larger $\Delta\Phi_2$. Hydrogen evolution thus limits the maximum flow rate through the porous cathode and therefore the useful electrode thickness, for given values of c_0 and κ.

It is assumed that the resistance loss in the carbon–copper matrix is small compared to that in the solution, and excess supporting electrolyte is assumed to be present in the solution.

Equations resulting from application of porous electrode theory [4] can be used to develop quantitative design procedures. When the electrode is operated at the limiting current, the material-balance relation within the porous cathode becomes

$$\frac{dc_b}{dy} = -\frac{ak_m}{v}c_b, \qquad (1)$$

where k_m is a mass-transfer coefficient for a

packed bed and is here assumed to be independent of y. At limiting current, this equation thus determines the reaction distribution. The current distribution is related to this reaction distribution by Faraday's law

$$\frac{di_2}{dy} = vnF\frac{dc_b}{dy}. \tag{2}$$

The potential distribution then follows from the current distribution by Ohm's law

$$i_2 = -\kappa\frac{d\Phi_2}{dy}. \tag{3}$$

As indicated above, the principle that determines the permissible flow rate and bed thickness is the allowable ohmic potential drop within the porous electrode, $\Delta\Phi_2$. This principle is a fairly general design concept for porous electrodes and other controlled potential electrolyses [5]. The potential difference between the carbon matrix and the solution, $\Phi_1 - \Phi_2$, should be sufficiently negative at all points within the porous cathode to ensure that copper deposition occurs at the limiting current but not so negative that there is appreciable evolution of hydrogen. The absolute value $|\Phi_1 - \Phi_2|$ is greatest at the front of the electrode, $y = 0$, and a minimum at the back of the electrode, $y = L$. Thus, one wishes to ensure limiting current at y equal L while avoiding hydrogen bubble nucleation at y equal zero. The difference in $\Phi_1 - \Phi_2$ between the front and back of the electrode is the potential variation in the solution, $\Phi_2^L - \Phi_2^O = \Delta\Phi_2$, assuming negligible potential variation in the solid matrix. If the effluent concentration is to be small, $\Delta\Phi_2$ can be estimated approximately as

$$\Delta\Phi_2 = 0(nFv^2c_o/ak_m\kappa).$$

Incidently, this relationship brings out the additional point that larger flow rates are permissible for solutions with a higher ratio of supporting electrolyte to reactant.

A cell might be designed to accommodate bubble evolution. However, such a design extension is beyond the scope of this study. For copper, an estimate of $\Delta\Phi_2$ equal $-0{\cdot}2$ V is reasonable.

The boundary conditions to Equations (1), (2), and (3) are

$$c_b = c_o \text{ at } y = 0 \tag{4}$$

$$i_2 = 0 \text{ at } y = L \tag{5}$$

$$\Phi_2 = 0 \text{ at } y = 0. \tag{6}$$

In these boundary conditions it is implicit that the backing plate or current collector is located at y equal L, the porous electrode-free solution interface is at y equal zero, and the anode is upstream of and opposite the cathode as shown in Fig. 1.

The solution to the equations, for which limiting current has been assumed, is

$$c_b = c_o \exp(-\alpha y) \tag{7}$$

$$i_2 = nFvc_o[\exp(-\alpha y) - c_b^L/c_o] \tag{8}$$

$$\Phi_2 = \beta[\exp(-\alpha y) - 1 + \alpha y c_b^L/c_o] \tag{9}$$

where

$$\alpha \equiv ak_m/v \tag{10}$$

$$\beta \equiv nFv^2c_o/ak_m\kappa. \tag{11}$$

Setting y equal zero in Equation (8) yields an expression for the overall current density:

$$i_T = nFvc_o(1 - c_b^L/c_o). \tag{12}$$

An ion recovery cell of this type will require specific operator attention when the cathode begins to plug and the cell is to be inverted, i.e., the cathode is made the anode and *vice versa*. If one assumes that the cathode becomes plugged when the porosity at the front of the cathode reaches half of its initial value, the time, t, that the cathode can be operated before the cell must be inverted is

$$t = \rho_{Cu}\varepsilon/2M_{Cu}ak_mc_o. \tag{13}$$

Before these equations can be used to design a cell, a method for estimating the mass-transfer coefficient k_m must be established. In the analysis presented here, k_m has been assumed to be independent of position y. Depending on the functional dependence of k_m on y (either implicitly or explicitly), revised solutions to the design equations may be found. For example, the pores can be assumed to be straight tubes and the Graetz analysis applied [6]. One then has to correct for tortuosity and porosity in later steps. The Graetz solution predicts an infinite mass transfer rate at the pore entrance. From Equa-

tion (13), it can be seen that if this were the case the pore openings would be plugged very quickly with copper. The experimental results indicate about 5 days operation prior to plugging. The constant k_m assumption (to be presented next) implies a plugging time of 49 days. Thus, it appears that a more realistic mass-transfer model lies between the extremes of the Graetz solution and a value of k_m independent of position.

Bird *et al.* [7] suggest a procedure for estimating k_m for Reynolds numbers below 50. However, the Reynolds numbers for the porous electrodes in this device are typically in the order of 3×10^{-3}. This Reynolds number range is at least an order of magnitude below the values for which the correlation suggested by Bird *et al.* has been tested. To illustrate the design procedure, however, the correlation suggested by Bird *et al.* will be used. That correlation is conveniently expressed in the form

$$\frac{k_m}{aD} = 0{\cdot}91\left(\frac{\rho v}{a\mu\Psi}\right)^{0.49} \Psi^2 Sc^{1/3} \qquad (14)$$

where Ψ is a shape factor, a the area per unit volume, and D the diffusion coefficient of copper ions.

The effective, overall conductivity in the electrolyte phase, κ, must be estimated from the bulk solution conductivity, κ^0. The equation proposed by de la Rue and Tobias [8] for a bed of packed spheres is suggested as a first approximation:

$$\kappa = \kappa^0 \varepsilon^{1{\cdot}5}. \qquad (15)$$

An example of a set of estimates of input parameters and resulting design characteristics is given in Table 1.

Table 1. Sample design calculation.

Input parameters		*Design results*
$c_0 = 667\ \mu g/ml$	$D = 6 \times 10^{-6}\ cm^2/s$	$v = 0{\cdot}0036$ cm/s
$c_b^L = 1\ \mu g/ml$	$\mu = 0{\cdot}01$ g/cm-s	$L = 4{\cdot}96$ cm
$\kappa^0 = 0{\cdot}17$ mho/cm	$\rho_{Cu} = 8{\cdot}92\ g/cm^3$	$i = 7{\cdot}29\ mA/cm^2$
$\varepsilon = 0{\cdot}3$	$M_{Cu} = 63{\cdot}5$ g/mol	$t = 49$ day
$\Delta\Phi_2 = -0{\cdot}2$ V	$Sc = 1670$	$\alpha L = 6{\cdot}5$
$a = 25\ cm^{-1}$	$\Psi = 0{\cdot}86$	$k_m = 1{\cdot}88 \times 10^{-4}$ cm/s
$\rho = 1\ g/cm^3$		

Experimental equipment and procedures

Cell construction

The experimental cell is shown in Fig. 1. The principal features are the two porous carbon electrodes (Union Carbide granules plus powder, GP-22). The carbon was irregularly shaped particles or flakes between 0·1 and 0·001 cm characteristic dimension. Each porous electrode was 10·1 cm diameter and 6 cm high. The electrodes were contained in a plexiglass body composed of two disk shaped end pieces, two tubular body sections, and a central ring separating the two electrodes. The feed entered through an opening in the central ring.

On the feed side of each electrode, the carbon flakes were contained by a 0·3 cm thick plexiglass plate drilled with 54 holes, 0·75 cm in diameter. The plexiglass support plate was backed by a sheet of Whatman 40 filter paper. The plexiglass support plate was held in place by a stainless steel rod through which the bed was compressed by tightening a nut pulling the rod through the end plate. The outlet side of the porous electrodes was contained by a 0·3 cm thick stainless steel plate containing 24 holes, 0·1 cm in diameter. The stainless steel also served as the electrical backing plate. Electrical connection was made to the stainless steel plate by a 0·3 cm diameter stainless steel rod threaded into the plate. The apparent density of the dry carbon bed was estimated to be 0·683 g/cm^3 with an

apparent porosity of 0·696 (including the internal porosity of the carbon particles).

There was a recess machined in each end plate providing a collection reservoir through which the product flowed to the product outlet ducts. Sealing was ensured by '0' rings. The four small locking nuts used inside the cell were aluminum.

Electrical circuit.

Commercial saturated calomel cells (Beckman) were placed in reservoirs in the feed and the two product streams. Thus, four independent potential measurements could be made: anode versus cathode (VA), feed calomel cell versus cathode (VF), dilute product calomel cell versus cathode (VDP), and concentrated product calomel cell versus cathode (VCP).

The circuit consisted of a potentiostat power supply (Anotrol Model 4700 M) with the control lead attached to the anode and the ground to the cathode. The power lead went to a resistor (1 Ω setting on Power Resistor Decade Box Model 240-C, Clarostat Mfg. Co.) and then to three ammeters in series (General Electric models 8DP9ACB1, 8DP9ACC1, and 8DP9ACM1) with varying ranges and then to the cell anode. The potential drop across the 1 Ω resistor was measured and recorded on a Sargent Model MR Recorder. The recorder was used to observe trends and establish when steady state was reached. The various ammeters checked one another to 2% or better. Readings were recorded from the ammeter with the most appropriate range.

The potential of the saturated calomel electrode in the dilute product stream versus the cathode (VDP) was measured on a Keithly Model 602 Electrometer and recorded on a Sargent Model SR Recorder with an attenuating adapter. The recorder was used to observe trends and establish when steady state was reached. The reported potential readings were made with a Hewlett-Packard Model 3440A Digital Voltmeter. Accuracy of both current and potential measurements was ±2%.

Flow control

The flow of the dilute product was controlled using a Nuclear Products Co. Micrometer Valve. The concentrated product was controlled using a needle valve. The relative variations in flow were measured with float type, glass flowmeters. Actual flow rates were determined using graduated cylinders to catch a known volume of product over a time period measured with a stop watch. Flow rates were adjusted so that variations were less than ±2%.

A gas vent and return line were installed on the feed distribution ring of the cell (not shown in Fig. 1).

The feed was stored in a 60 l plastic tank, the bottom of which was 1 m above the cell. Flow was by gravity.

Solution concentrations

Feed and product concentrations were measured using a Perkin Elmer Model 303 Atomic Absorption Spectrophotometer. Concentrations below 20 μg of Cu per ml of solution were measured directly, after calibrating the readings. Higher concentrations were diluted by volume to the 20 μg/ml range. Above 1 μg/ml, accuracy was about ±5% as determined by running known, calibrated solutions. Below 1 μg/ml the accuracy was about ±0·1 μg/ml since this was approximately the noise level generally encountered.

The feed contained sodium sulfate as supporting electrolyte at a concentration of 0·8 M. The feed pH was adjusted to between 2·5 and 2·6 by adding sulfuric acid. The feed and product conductivities were measured using a Leeds and Northrup Electrolytic Conductivity Bridge, catalog number 4959, and an Industrial Instruments (Cedar Grove, N.J.) conductivity probe with cell constant 2·00 cm^{-1}. The feed conductivity varied between 0·16 and 0·19 mho/cm, depending on temperature. Other than the room air conditioning, no temperature control was used on the feed. The feed temperature varied between 21 and 24°C.

Cell orientation

The cell was, at various times, oriented as shown in Fig. 1 and 90° to the position shown. When on its side, bubbles more easily escape through

the vent (not shown). However, if the anolyte flow is low, giving the desired high anolyte effluent copper concentration, natural convection will cause concentrated copper solution to flow from the anode to the cathode, i.e., the product streams are mixed. This mixing makes proper operation of the cell impossible. Thus, the orientation of cathode over anode shown in Fig. 1 is necessary.

Electrode packing

The electrode that is initially to be the anode must have a sufficient quantity of fine copper powder placed in the porous electrode packing to allow continuous copper dissolution during the first cycle. If this is not done, oxygen evolution and undesirable pH changes will result. When the anode is switched to the cathode, excess copper powder in the porous electrode does not seem to affect the operation of the new cathode. Several cell inversions, switching anode for cathode, were accomplished successfully. Only one failure occurred. The electrode, initially the anode, was packed with some copper screen as well as fine copper powder. The screen warped during packing, creating some open 'pockets' in the electrode structure. The screen only partly dissolved during its anodic service. While this electrode was the cathode, massive copper deposits formed around the remnants of the copper screen. These deposits formed a dome, prematurely plugging the electrode. Only fine copper powder should be used in making the first cycle anode. The electrodes should be carefully and tightly compacted to prevent open pockets, provide good matrix phase electrical conductivity, and to prevent channeling of the flow.

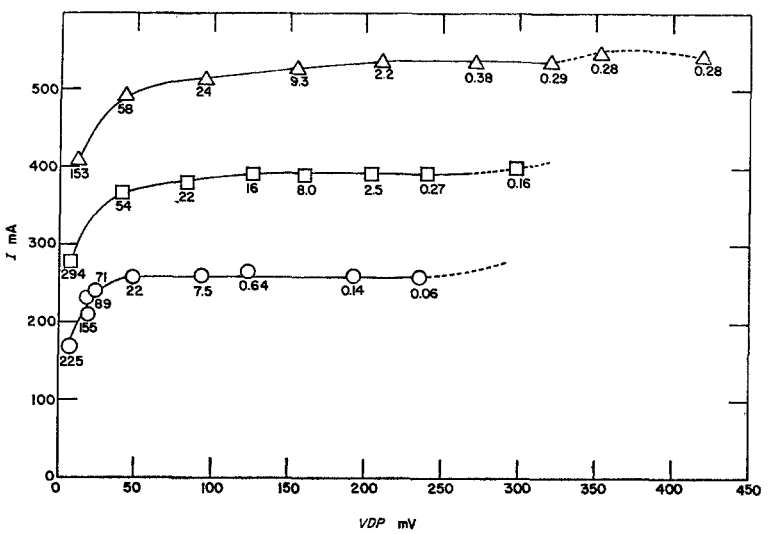

Fig. 2. Limiting current curves. Superficial electrode area = 80 cm^2. ○ 8 cm^3/min dilute product flow and 637 μg of Cu/ml of feed. □ 12 cm^3/min dilute product flow and 642 μg of Cu/ml of feed. △ 16 cm^3/min dilute product flow and 667 μg of Cu/ml of feed. Numbers below points are dilute product concentration in μg of Cu/ml of solution. Dashed lines imply region in which gassing was observed. VDP is the potential of a saturated calomel cell in the dilute product stream versus the cathode.

Materials compatibility

On one preliminary run, the Whatman 40 filter paper was replaced by a fine mesh stainless steel screen. On anodic operation, the screen was completely corroded away. However, the heavy stainless steel backing plates did not show signs of deterioration over 2½ months of operation. The four aluminum hold-down nuts used inside the cell did not show signs of deterioration. Thus, it may be possible to replace the stainless steel backing plates, tie rods, and electrical connectors with suitable aluminum or aluminum alloy material.

When electrically conducting stainless steel face plates were used on the feed side of the porous electrodes, premature hydrogen evolution, early cell plugging, and dendrite formation and associated shorting occurred. The plastic face plates tended to crack if too much stress was applied in assembling the electrodes. However, once assembled with the plastic face plates, satisfactory cell operation was realized.

Results

Fig. 2 shows the limiting current and dilute product concentrations for various flow rates through the cathode. The feed concentration increased slightly from run to run due to evaporation from the feed tank. Approximately 1 to 2 hr were required to reach a true steady state after each change in the control potential, VA. Steady state was easily observed to exist when the total current and VDP stopped varying and remained constant. There was normally a rounded break in the slope of these curves when steady state was reached. Points were independent of whether VA was being increased or decreased.

A total of 97·5 l of feed solution containing between 600 and 670 μg of Cu per ml of solution were processed over a total of 131 hr of operating time. During the last 67 hr, 49 l of feed were processed continuously with operator attention only for about 15 min, twice a day. The run was terminated when a flow rate of 9·5 cm^3/min was all that could be maintained with the dilute product flow control valve wide open. There was some floc in the feed as a result of dust which collected in the feed over several weeks. This may have contributed to the plugging. The average dilute product concentration collected during the final 67 hr was 0·55 μg of Cu per ml of solution. During the same period, 0·54 l of concentrated product was collected with an average concentration of 0·74 M in copper sulfate.

Operating Guidelines

Bubble formation

Once bubbles start to form, they eventually break away and exit via the vent in the feed ring. As the bubbles form, the cell potential VA must increase (possibly several hundred millivolts) to compensate for increased resistance losses. As bubbles break away and exit through the vent, large local shifts in potential driving force occur at the electrode because of local changes in resistance losses in the solution. In some cases it was observed that these transients apparently resulted in local potential driving forces sufficient to cause reduction of sulfate ions. This reduction resulted in H_2S formation and precipitation of copper sulfide. Besides the unpleasant odor of the H_2S, the copper sulfide precipitate began plugging the electrode and compounding the nonuniformity of current distribution.

Within 10 to 20 min, under these copper sulfide forming conditions, the electrode became so plugged that operation was stopped. Although the effluent under these conditions was below 1 μg/ml in copper, the black precipitate was plugging the control valve and flow meter. Gentle to strong flushing with sulfuric acid solution was sufficient to restore the cell to operating condition at a lower value of VDP. Unless a cell is specifically designed for continuous, smooth removal of gas bubbles, porous-electrode cells of this type should not be operated while gassing.

Cell control

Control of the cell must be careful and deliberate. The superficial residence time for fluid going through the cathode is 30 min. For large changes in operating conditions, such as occur at start up, transient responses of 1 to 2 hr are to be expected. A variety of potential control modes were tried. The potential VDP is the most descriptive of how well the cell is removing copper. The higher VDP, the lower the cathode effluent copper concentration (see Fig. 2). However, when the potentiostat control lead was attached to the VDP lead, cell operation became unstable. The current began to fluctuate ± 2A and greater, including excursions into hydrogen evolution and sulfide forming regions. This type of control does not work. Attaching the potentiostat control lead to the feed reference electrode, VF, was fairly satisfactory. However, small bubbles,

flakes of carbon, *etc.* would occasionally lodge near the feed entrance and change local resistance losses. The resulting shift in control point would upset the cell operation. The best control technique was to connect the potentiostat control lead to the anode and simply control the cell potential VA to achieve a desired VDP. The potential VDP responds very slowly to changes in VA. An increase in VA will yield an approximately proportional steady state change in VDP. However, VDP may go through some oscillations before becoming steady. Large, rapid changes in VA should be avoided. After a small change in VA, 30 min to 2 hr should be allowed before drawing a conclusion about the resulting effect on the steady state cell operation. Since the overall cell potential is the directly controlled variable, a potentiostat power supply is not needed. A power supply giving a controllable output potential should be sufficient. For a flow of 16 cm^3/min with a cell area of 80 cm^2, a copper feed concentration of 667 μg/ml, a feed conductivity of 0·17 mho/cm, and a VDP of 273 mV, the cell potential VA was 1·22 V.

Flow control appears to be important. As an illustration, suppose that the catholyte flow control valve should stick in a fixed position. As the cathode slowly plugs, the catholyte flow will slowly decrease. This will cause a slow increase in VDP. If one was initially operating near the economic maximum close to hydrogen evolution, the described sequence of events will send the cell into the hydrogen evolution domain (see Fig. 2).

Electrode plugging

The theoretical model predicted a 49 day life before the face of the cathode became plugged with copper. The observed cycle life was 5·5 days. This difference is probably due to a low estimate of k_m at the electrode face. However, the time to plugging is probably dependent on the amount of particulates in the feed as well as the copper deposition distribution. There was considerable dust in the feed near the end of the final run. Three to seven days seems to be a reasonable estimate for cycle life under the operating conditions studied.

Discussion

Comparison of theory and experiment

The cell design shown in Table 1 is an attempt to predict the cell operating characteristics for the experimental conditions used. The observed flow rate of 0·0033 cm/sec compares well with the predicted flow rate of 0·0036 cm/sec as the maximum flow rate allowable while still maintaining 1 μg/ml or less copper in the product stream. Fig. 2 shows that the curve for 16 cm^3/min (same as 0·0033 cm/s) reaches the dilute product design concentration of 1 μg/ml at about VDP equal 250 mV. This is getting close to the potential at which hydrogen evolution was observed. For higher flow rates it is to be expected that as VDP is increased hydrogen evolution will occur before the dilute product reaches the design specification of 1 μg/ml.

Curve shapes

The potential of the abscissa of Fig. 2 is, to a good approximation, the potential in the solution at the back of the cathode, Φ_2^L. As discussed in the Design Principles section, it is the potential in the solution at the front of the cathode, Φ_2^0, that controls hydrogen evolution, i.e., VDP minus $\Delta\Phi_2$. As the flow rate is increased, I increases. Thus, if the solution resistance remains constant, one might expect $\Delta\Phi_2$ to become more negative and gassing to occur at lower values of VDP as the flow is increased. The results shown in Fig. 2 indicate that the opposite occurs. This may be fortuitous, but some explanation seems desirable.

It is not hydrogen evolution itself that causes trouble, rather bubble nucleation. If 0·000158 g of H_2 per 100 g of water must dissolve in the catholyte before nucleation takes place [9], this implies that at 8 cm^3/min, 20 mA of current must go to hydrogen production before bubble nucleation occurs. At 16 cm^3/min, 40 mA must go to hydrogen evolution to initiate bubble nucleation. It can be seen from Fig. 2 that between 20 and 40 mA is the correct order of magnitude for the current going to gassing. Thus, it seems reasonable, tentatively, to propose that operation without gassing can be

sustained at higher values of VDP at higher flow rates because bubble nucleation is delayed due to higher rates of removal of dissolved hydrogen.

The decrease in current at VDP equal 422 mV for a flow of 16 cm^3/min is probably due to bubbles increasing resistance losses in front of the cathode, blocking some of the electrode, and decreasing the effective electrical driving force.

Cost analysis

Accurate cost estimates will depend on size and details of the design and materials of construction. These details will depend on the feed, particularly its corrosion properties. However, a very approximate cost estimate may be helpful as a beginning basis for judging the practical utility of the fixed bed, electrochemical removal of copper ions.

A realistic pilot plant of 48 ft^2 (4·46 m^2) effective cathode operating area has been designed. The cell is constructed of plywood with asphalt coating on the inside and acid-resistant epoxy paint on the outside. A wooden frame is included for mounting the cells. No allowance is made for taxes or for building space in which the unit may be located. The pilot unit is capable of processing 2·33 gpm (8·82 l/min) or $1{\cdot}24 \times 10^6$ gal/yr (4.70×10^6 l/yr) of feed containing 600 μg/ml of copper. A total of 6,230 lb/yr (2,820 kg/yr) of copper will be recovered. The cost of the pilot size unit is estimated to be \$1,264 or \$26.40/ft^2 (\$2.45/m^2). Assuming a five-year straight-line depreciation and 12% return on invested capital, the operating costs are estimated to be:

capital cost	\$328.65/yr	\$0.265/kgal
operating labor	52.00	0.042
electrical energy	41.10	0.033
pumping	0.18	—
Total	\$422.00/yr	\$0.34/kgal

Assuming the recovered copper is worth \$0.10/lb in the concentrated effluent, \$623/yr of copper is recovered or a net profit of \$201/yr. The profit per unit of electrode area is \$4.19/ft^2 (\$0.16/kgal) in addition to an average of 12% interest returned on the invested capital. Assuming that cell capital costs increase as the 0·6 power of the cell size in terms of design throughput, the cost per unit area will decrease to \$4.20/ft^2 for a unit 100 times larger than the pilot unit. If operating labor also increases with the 0·6 power of the throughput, the operating costs become \$0.082/kgal. A value of \$0.50/kgal of copper recovered still applies. Thus, a net profit of \$0.42/kgal of feed processed in addition to 12% interest on invested capital could be realized for an installation capable of handling 233 gpm of feed.

Cost calculations of this general nature are of necessity quite approximate. The cost picture will change depending on the exact nature of specific problems. However, these approximate cost estimates suggest that the concept may be economically attractive in some situations.

Other applications

The method should also work well for recovery of Au, Ag, Hg, Pb, and Cd. Its use for Zn, Cr, As, or Mn recovery may be possible. But since these metals deposit in potential regions where hydrogen gassing is likely, more difficulty is to be expected.

The general operational scheme is that of a concentrating device. It can be used for metal recovery from dilute solutions. It can also be used for trace metal analysis. For example, 100 l of sea water could be processed through the cathode electrode. Whatever is deposited can then be stripped off anodically into 0·1 to 1 l of anolyte. The resulting solution will contain the electropositive ions concentrated 100 to 1,000 times. For example, electropositive ions such as Hg initially present at possibly 0·01 ppm would be 1 to 10 ppm in the concentrated anolyte solution. There are many analytical techniques which can then be used for analysis in the 1 to 10 ppm range.

Acknowledgment

This work was supported by the University of California.

List of Symbols

a area per unit volume, cm^{-1}

c_o copper concentration of feed, mol/cm^3

c_b averaged, bulk copper concentration within porous cathode, mol/cm^3
c_b^L copper concentration in cathode effluent, mol/cm^3
D diffusion coefficient of copper ions, cm^2/s
F Faraday's constant, 96,487 coul/equiv
i_2 superficial or overall electrical current density in catholyte solution, A/cm^2
i_T total, overall current density to cathode, A/cm^2
I total current, mA
k_m mass transfer coefficient, cm/s
L thickness of the cathode, cm
n number of electrons transferred in electrode reaction, 2
Sc Schmidt number $\mu/\rho D$, dimensionless
t time to plug cathode with copper, s
v superficial or approach velocity of catholyte solution, cm/s
VDP potential of saturated calomel reference electrode in catholyte effluent relative to the cathode, V
VA potential of anode relative to cathode, V
y distance from entrance of cathode toward cathode backing plate, cm
α ak_m/v, cm^{-1}
β $nFv^2c_o/ak_m\kappa$, V
ε void fraction, dimensionless
κ effective or superficial electrical conductivity of catholyte, mho/cm
κ^o electrical conductivity of feed solution, mho/cm
μ viscosity of feed solution, g/cm-s
ρ density of feed solution, g/cm^3
Φ_2 potential in the solution, V
Ψ particle shape factor, 0·86 for flakes, dimensionless

References

[1] N. A. Lange, editor, 'Handbook of Chemistry', eighth edition, p. 788, Handbook Publishers, Inc., Sandusky, Ohio (1952).
[2] J. E. Browning (News Editor), *Chem. Engr.*, **78** April 19 (1971) 62.
[3] M. Fleischmann, J. W. Oldfield and L. Timakoon, *J. Appl. Electrochem.*, **1** (1971) 103.
[4] J. S. Newman and C. W. Tobias, *J. Electrochem. Soc.*, **109** (1962) 1183.
[5] W. H. Smyrl and J. Newman, submitted to *J. Electrochem. Soc.* (UCRL-20380, Feb. 1971).
[6] J. Newman, 'The Graetz Problem', UCRL-18646. Berkeley: Lawrence Radiation Laboratory, University of California (1969).
[7] R. B. Bird, W. E. Stewart and E. N. Lightfoot, 'Transport Phenomena', pp. 411 and 679, John Wiley & Sons, Inc., New York (1960).
[8] R. E. de la Rue and C. W. Tobias, *J. Electrochem. Soc.*, **106** (1959) 827.
[9] N. A. Lange, *loc. cit.*, p. 1082.